Compartmentalized control of Cdk1 drives mitotic spindle assembly.

Angela Flavia Serpico[1,2], Francesco Febbraro[1,2], Caterina Pisauro[1,2] & Domenico Grieco[1,3*].
[1]CEINGE Biotecnologie Avanzate, Naples, Italy; [2]DMMBM, University of Naples "Federico II", Naples, Italy; [3]Department of Pharmacy, University of Naples "Federico II", Naples, Italy.

*Correspondence and requests for materials should be addressed to D. G. (email: domenico.grieco@unina.it).

Abstract

During cell division, dramatic microtubular rearrangements driven by cyclin B-cdk1 (Cdk1) kinase activity mark mitosis onset leading to interphase cytoskeleton dissolution and mitotic spindle assembly. Once activated by Cdc25, that reverses inhibitory phosphorylation operated by Wee1/Myt1, Cdk1 clears the cytoplasm from microtubules by inhibiting microtubule associated proteins (MAPs) with microtubule growth-promoting properties. Nevertheless, some of these MAPs are required for spindle assembly, creating quite a conundrum. We show here that a Cdk1 fraction bound to spindle structures escaped Cdc25 action and remained inhibited by phosphorylation (i-Cdk1) in mitotic human cells. Loss or restoration of i-Cdk1 inhibited or promoted spindle assembly, respectively. Furthermore, polymerizing spindle microtubules fostered i-Cdk1 by aggregating with Wee1 and excluding Cdc25. Our data reveal that spindle assembly relies on compartmentalized control of Cdk1 activity.

To prevent chromosome damage during spinlde assembly, the microtubular interphase cytoskeleton must be dismantled at the onset of mitosis and, as many mitotic features, this is an event downstream Cdk1 activation. Indeed, Cdk1 activity clears cytoplasmic microtubules by directly or indirectly affecting several microtubule-stabilizing and -destabilizing MAPs, inhibiting, for instance, the microtubule growth-promoting properties of ch-Tog and Map4 (*1, 2, 3, 4, 5*). Nevertheless, a number of these MAPs are required for spindle microtubule growth (*2, 6, 7*). Thus, how spindle assembles despite the potent microtubule-destabilizing action of Cdk1 is unknown. During interphase, Cdk1, accumulates in an inactive state, phosphorylated at inhibitory sites by Wee1/Myt1 kinases (*8*). At mitosis onset, initial reversal of these phosphorylation by Cdc25 phosphatase is rapidly followed by full Cdk1 activation via positive feedback loops in which Cdk1 inhibits Wee1/Myt1 and stimulates

35 Cdc25 (*8*). Thus, inhibitory phopshorylation of Cdk1 has a crucial role in ensuring completion of
36 interphase tasks before mitosis onset, but once Cdk1 activation begins this control appears to be
37 rapidly suppressed by autoactivatory feedback loops. Cdk1 is believed to be only inactivated upon
38 spindle assembly by cyclin B degradation (*8*). Nevertheless, early evidence indicated that cells
39 expressing a Cdk1 version non-phosphorylatable at the inhibitory sites threonine 14 and tyrosine 15
40 (Cdk1AF), rapidly entered mitosis but failed to assemble spindles (*9*). These mitotic defects were,
41 however, ascribed to premature mitosis onset in presence of incompletely replicated DNA and not as
42 a requirement for inhibitory phosphorylation of Cdk1 in spindle assembly (*9*). In addition, evidence
43 that i-Cdk1 is present in meiotic and mitotic extracts from Xenopus eggs and mouse eggs was later
44 reported (*10, 11*). Here we examined if and how inhibitory phosphorylation of Cdk1 had a role for
45 spindle assembly.
46
47 To this end, we begun analysing spindle assembly upon downregulation of Wee1 expression by small
48 interfering RNAs (siRNAs) in hTERT-RPE1 cells. To prevent premature mitosis onset upon Wee1
49 downregulation, 6 hours post Wee1-siRNA treatment cells were incubated with the selective and
50 reversible Cdk1 inhibitor RO-3306 at 9 μM (high-RO) for further 16 hours, to allow completion of
51 DNA replication and arrest cell cycle at G2 (*12)*. As control, part of Wee1-siRNA-treated cells were
52 previously complemented with siRNA-resistant Wee1 expression vector (fig. 1A; Fig. S1) (*13*). Upon
53 release from G2-arrest into fresh medium, containing the proteasome inhibitor MG-132 to block
54 mitosis exit and the protein synthesis inhibitor cycloheximide to prevent abnormal protein
55 accumulation (M/C medium), the majority of control cells built normal bipolar spindles within 60
56 min incubation, that remained stable for further 20 min incubation (fig. 1A). Conversely, spindle
57 assembly was markedly impaired in Wee1-downregulated cells, with defects that ranged from
58 monopolarity to poorly structured bipolar spindles with gross chromosome alignment abnormalities
59 (fig. 1A). To establish whether impaired spindle assembly was due to Wee1 loss *per se* or because it
60 affected Cdk1 activity, we asked if mild Cdk1 inhibition could restore spindle assembly in Wee1-
61 downregulated cells. Indeed, addition of RO-3306 at 0.5 μM (low-RO), from 60 to 80 min post G2
62 release, substantially restored spindle assembly (fig. 1A). Defects in spindle assembly were also
63 induced by cdk1AF overexpression under similar conditions of G2-arrest and release, paralleling
64 what described by Krek and Nigg in 1991, as well as in Wee1-siRNA-treated HeLa cells or by
65 chemical inhibition of Wee1, in all cases defects were substantially reversed by low-RO (figs. S2, S3
66 and S4A) (*9, 14)*. In another set of experiments, non-targeting-siRNA-, as control, and Wee1-siRNA-
67 treated hTERT-RPE1 cells were arrested at prometaphase by the reversible microtubule inhibitor
68 nocodazole added shortly after siRNA treatments (as described in Materials and Method). Cells were,

69 then, released in M/C medium for 80 min and a portion of Wee1-siRNA-treated cells also received
70 low-RO at 60 min incubation. Within this period, the majority of control cells assembled spindles,
71 while assembly was strongly impaired in Wee1-siRNA-treated cells but restored by low-RO (fig.
72 1B). When cells were released just into fresh medium, mitosis exit was delayed in Wee1-siRNA-
73 treated cells, as shown by delayed cyclin B1 degradation, presumably by the action of the spindle
74 assembly checkpoint (SAC; fig. S5) (*15)*. Together, these data suggest that inhibitory
75 phosphorylation-dependent control of Cdk1 activity is required for spindle assembly.
76
77 To directly test if i-Cdk1 was present in mitotic cells and where it was localised, we probed metaphase
78 cells with an antibody recognizing cdk1 phosphorylated at tyrosine 15 (p-Y15-cdk1; fig. 2A). The p-
79 Y15-cdk1 signal appeared decorating the spindle area paralleling total cdk1 localization (fig. 2A). To
80 biochemically dissect localization and function of mitotic i-Cdk1, we adapted a method described by
81 Nigg and coworkers to isolate mitotic spindles and tightly associated proteins by separating
82 microtubular, insoluble, pellet fraction (P) from soluble fraction (S) of mitotic cells (see Materials
83 and Methods) (*16*). Nocodazole-treated, prometaphase-arrested hTERT-RPE1 cells (Pro) were
84 collected and taken at time 0 or taken after release in M/C medium for 60 min to have metaphase-
85 arrested cells (Meta; fig. 2B). Cells were fractionated and proteins from S and P fractions analyzed
86 (fig. 2B; P fraction was enriched 4 folds relatively to S fraction). In Pro cell P fraction, centrosomes
87 were present as indicated by significant amounts of the central protein γ-tubulin and Nuclear and
88 Mitotic Apparatus protein 1 (NuMA1), a centrosome-associated protein (fig. 2B) (*3*). Conversely, α-
89 tubulin was substantially present in S fraction and much less in P fraction, as expected because of the
90 microtubule polymerization block, as well as the MAPs Map4 and ch-Tog (fig. 2B). In Meta cells,
91 instead, α-tubulin and significant amounts of Map4 and ch-Tog, the latter also involved in activating
92 centrosome-independent, intra-spindle, microtubule nucleation, were present in P fraction, reflecting
93 spindle assembly (fig. 2B) (*17, 18*). Distribution of NuMA1 and γ-tubulin in S and P fractions did not
94 substantially change between Pro and Meta cells (fig. 2B). P fraction also contained small amounts
95 of Wee1 that increased in Meta cells, while minimal amounts of Cdc25C were equally present in P
96 fraction of both Pro and Meta cells (fig. 2B; similar protein distribution was found in HeLa cells
97 under similar experimental conditions; see Fig. S6). Small amounts of cyclin B1 and cdk1 were
98 present in P fraction of Pro cells and more of Meta cells (fig. 2B). However, i-Cdk1 was found quite
99 exclusively in P fractions, as shown by p-Y15-cdk1 signal and by retarded cdk1 mobility on
100 SDS/PAGE, and more from Meta than from Pro cells (Fig. 2B) (*19*). Quantitation of the upshifted
101 cdk1 forms from Meta cell P fraction indicated that i-Cdk1 represents less than 10% of total Cdk1.
102 The selective presence of i-Cdk1 in P fraction was confirmed also by probing immunoprecipitates

103 (Ips) of comparable amounts of cyclin B1 from S and P fraction of Meta cells (Fig. 2C). In Meta cell
104 P fraction, Map4 and ch-Tog appeared to have increased mobility on SDS/PAGE compared to S
105 fraction, suggesting that these proteins were relatively dephosphorylated when microtubule-bound.
106 Indeed, when Meta cells were further treated with nocodazole, from 60 to 80 min, to revert to a
107 prometaphase condition, distribution of proteins between S and P fractions returned similar to Pro
108 cells; Map4 and ch-Tog regained slower migration on SDS/PAGE, presumably reflecting their re-
109 phosphorylation when returning into the cytoplasm, while Wee1 and i-Cdk1 were reduced in the P
110 fraction, indicating their dependence also on microtubule polymerization (fig. 2D).
111
112 To ask whether a cause/effect relationship existed between i-Cdk1 and the control of Map4 and ch-
113 Tog dephosphorylation and distribution, prometaphase-arrested control and Wee1-siRNAs were
114 released into M/C medium as described in Fig. 1b. Cells were further fractionated and the S and P
115 fractions analyzed (fig. 2E). Control cells showed a similar distribution as in Meta cells described in
116 Figs. 2b, d. In Wee1-siRNA-treated cells the distribution of γ-tubulin and NuMA1 between the S and
117 P fractions were similar to control cells, however, Map4, ch-Tog and even part of α-tubulin were
118 substantially less present in the P fraction relatively to control cells, a distribution pattern similar to
119 that of Pro cells described in figs 2A, D (fig. 2E). Addition of low-RO to Wee1-siRNA-treated cells
120 reversed protein distribution relocating Map4, ch-Tog and α-tubulin from S to P fraction similarly to
121 control cells (fig. 2E). As expected, i-Cdk1 was reduced in Wee1-dowregulated cell P fraction
122 compared to controls, however, addition of low-RO induced accumulation of part of residual Wee1,
123 that escaped siRNA-mediated downregulation, in P fraction and restored i-Cdk1 content (fig. 2E;
124 note Wee1 in short, SE, and long exposures, LE). No increase of p-Y15-cdk1 signal was detected in
125 S fraction upon low-RO addition, indicating that small fluctuation of Cdk1 activity are indeed
126 buffered in the cytosol by strong hysteresis and bistability of the Cdk1 autoactivatory loops, while
127 nucleating spindle microtubules appeared insulated from them (fig. 2E) (*8, 20, 21*). Localized
128 inhibition of endogenous Cdk1 by low-RO treatment, could possibly explain spindle assembly
129 restoration in cdk1AF-expressing cells (fig. S2). Immunofluorescence (IF) analysis confirmed that
130 the two MAPs poorly localised to defectively structured spindles in Wee1-downregulated cells in a
131 low-RO-reversible manner (fig. 2F). Similar mitotic defects and changes in protein distribution were
132 induced by the chemical Wee1 inhibitor AZD1775 upon release from prometaphase-arrest, also in
133 this case corrected by low-RO (fig. S4B). Together, these data indicate that i-Cdk1 is required for
134 proper mitotic spindle assembly and spindle microtubule association of Map4 and ch-Tog.
135

136 Microtubule growth- and stability-promoting properties of MAPs like ch-Tog and Map4 are
137 antagonized by direct Cdk1 phosphorylation (*2, 3, 4, 5, 6*). We were intrigued by the fact that changes
138 in migration on SDS/PAGE suggested that these MAPs were hypophosphorylated when associated
139 with spindle microtubules (fig. 2B, D). We developed an anti-phosphospecific antibody recognizing
140 phosphorylated Map4-serine 787 (p-S787-Map4), a target site for inhibition by Cdk1 *in vivo* (*22*).
141 Indeed, when the fusion proteins tGFP-Map4-wild type (WT) and tGFP-Map4-S787A (S787A), in
142 which Map4 serine 787 was mutated into non-phosphorylatable alanine, were expressed and isolated
143 from mitotic cells, the antibody recognized wild type but not the mutant version (fig. S7). Probing
144 Ips of comparable amounts of endogenous Map4 from S and P fractions of Meta cells for p-S787-
145 Map4 showed that the signal was readily detected from S fraction while hardly from P fraction (fig.
146 3A). In addition, treating P fraction Map4 with active Cdk1, *in vitro*, restored strong p-S787-Map4
147 signal and slower Map4 migration (fig. 3B). These data indicate that Map4 is dephosphorylated at
148 Cdk1-dependent sites when bound to microtubules. Map4 and ch-Tog have been shown to physically
149 interact with Cdk1, mediating association of the kinase with microtubules (*6, 23*). Our data from
150 Wee1 downregulation experiments suggested that ch-Tog and Map4 distribution in the P fraction
151 depended on i-Cdk1. Indeed, Ips of comparable amounts of Map4 or ch-Tog from the S and P fraction
152 of Meta cells showed that the MAPs selectively interacted with Wee1 and i-Cdk1 in P fraction (figs.
153 3C, D). Together, these observations suggest that the interaction of microtubule-associated MAPs
154 with i-Cdk1 was instrumental for their dephosphorylation (fig. 3A, C, D). In mitosis, major protein
155 phosphatases like PP1 and PP2A are directly or indirectly inhibited by Cdk1 (*1*). PP1 catalytic subunit
156 is directly inhibited by Cdk1 phosphorylation, in particular the alpha isoform, PP1α, at threonine 320
157 (p-T-320-PP1α) and phosphorylation in analogous sites inhibits other PP1 isoforms (*24*). PP1 can,
158 however, rapidly autoactivate by dephosphorylating itself, provided no Cdk1 activity in the proximity
159 (*24*). In addition, PP1 often interacts with its substrates through specific domains (*25*). Thus, first we
160 asked whether PP1 interacted with Map4 and ch-Tog and found that the MAPs interacted with PP1α
161 only in the P fraction (figs. 3C, D). Because of the presence of i-Cdk1, we hypothesised that PP1α in
162 P fraction was dephosphorylated at the Cdk1 inhibitory site. Indeed, when comparable amounts of
163 PP1α were analyzed from S and P fractions of Meta cells, the p-T-320-PP1 signal was substantially
164 detectable in S fraction and barely in P fraction (fig. 3E). In addition, probing comparable amount of
165 PP1α from total S fraction and from Map4 and ch-Tog Ips showed that MAP-associated PP1α was
166 dephosphorylated at the inhibitory Cdk1-dependent site (fig. 3F). Moreover, active PP1α was able to
167 dephosphorylate Map4-S787 *in vitro* (fig. 3G). Together, these data suggest that i-Cdk1 coopts active
168 PP1 to reverse inhibitory phosphorylation of Map4 and ch-Tog, and possibly other MAPs, for spindle
169 microtubule growth. When prometaphase-arrested control-siRNA- and Wee1-siRNA-treated cells

170 were released into M/C medium for 80 min, PP1α was readily detectable in Map4 and ch-Tog Ips
171 from total extracts of control but not of Wee1-siRNA-treated cells (fig. 3H, lane 6). Addition of low-
172 RO to Wee1-siRNA-treated cells, that restored i-Cdk1 and spindle assembly (see fig. 2E), also
173 restored efficient PP1α binding to Map4 and ch-Tog (fig. 3H, lane 9). Thus, i-Cdk1 allowed Map4
174 and ch-Tog interaction with active PP1 to promote their dephosphorylation. The Map4 sequence
175 KDVRW (from aa 318 to 322) matched a rather conserved PP1 binding motif (R/KxVxF/W; where
176 x is any aa) (*25*). We mutated it into KDARA in tGFP-Map4-WT expression vector to produce tGFP-
177 Map4-PP1-KO, a mutant impaired in PP1 binding. Indeed, when tGFP-Map4-WT and tGFP-Map4-
178 PP1-KO were expressed at comparable levels and isolated from Meta cells, PP1α substantially bound
179 tGFP-Map4-WT but not tGFP-Map4-PP1-KO (figs. 3J, K). When the distribution in S and P fractions
180 of tGFP-Map4-WT- and tGFP-Map4-PP1-KO-transfected Meta cells was analyzed, tGFP-Map4-WT
181 was readily detectable in the P fraction while tGFP-Map4-PP1-KO remained substantially in S
182 fraction (fig. 3I). We concluded that i-Cdk1 is required for spindle localized interaction of
183 microtubule-stabilizing MAPs with active PP1 and for PP1-dependent reversal of their inhibitory
184 phosphorylations, operated by Cdk1 and other mitotic kinases, in order to locally restore their
185 microtubule growth-promoting properties.
186
187 Probing the cyclin B1 Ips form S and P fractions of Meta cells, shown in fig. 2C, for γ-tubulin revealed
188 that it interacted with Cdk1 in P fraction (fig. 4A). Conversely, probing γ-tubulin Ips from S and P
189 fraction of Pro cells showed that it selectively interacted with i-Cdk1 and Wee1, in P fraction (fig.
190 4B). In Meta cells P fraction, i-Cdk1 and Wee1 increased relatively to the P fraction of Pro cells,
191 suggesting a mutual relationship between microtubule polymerization and i-Cdk1 formation (see figs.
192 2B, D and 3C, D). This may reflect further Wee1 recruitment and i-Cdk1 formation at intra-spindle
193 microtubule nucleation points, in a γ-tubulin-dependent manner, but also further i-Cdk1 formation by
194 growing spindle microtubules, in a mutual fashion, as suggested by the interaction of i-Cdk1 with
195 Map4 in Meta cell P fraction (see fig. 3C) (*17, 18*). When the repartition of the Cdk1 inhibitory
196 pathway players between S and P fractions in Pro and Meta cells was probed on blots where the P
197 fraction was enriched 10 folds over the S fraction, it appeared more evident that the increase of Wee1
198 in P fraction of Meta cells relatively to Pro cells was microtubule-dependent, Myt1 also increased
199 albeit to a lesser extent (fig. 4C). No changes in distribution between fractions in Meta and Pro cells
200 were, instead, detected for Cdc25 phosphatase family members (fig. 4C). Thus, polymerizing spindle
201 microtubules appeared to bind Wee1 but not with Cdc25, further promoting i-Cdk1 insulated from
202 the cytoplasmic Cdk1 autoactivatory loops (fig. 4C) (*8, 20, 21*). To corroborate the hypothesis that
203 nucleating microtubules compartmentalized the Cdk1 control fostering i-Cdk1 formation, we used

204 concentrated cytoplasmic cell extracts from prometaphase-arrested HeLa that were incubated with
205 nocodazole or with the microtubule stabilizer taxol for 20 min at 23ºC, the pellets were then eluted
206 and analyzed (*25*). The microtubular pellets aggregated with Wee1 and i-Cdk1 but not with Cdc25
207 family members (fig. 4d). The presence of Wee1 on spindles in cells was also confirmed by IF (fig.
208 4E). Thus, in mitosis, positive feedback loops keep Cdk1 active in the cytoplasm to clear peripheral
209 cytoplasmic microtubules by phosphorylating MAPs for safe chromosome movements and possibly
210 to destabilize spindle microtubules that do not, or weakly, bind chromosomes (fig. 4F). At the same
211 time, centrosomes, and perhaps intra-spindle γ-tubulin nucleating centers, along with their nucleating
212 microtubules foster localized i-Cdk1 for PP1-dependent reversal of inhibitory MAP phosphorylation
213 and spindle microtubule growth (fig. 4f) (*3, 17, 18, 27*). Compartmentalized control of Cdk1 activity
214 might also be contributed by other mechanisms in addition to inhibitory phosphorylation of Cdk1 and
215 relevant to terminate the SAC-sustaining action of Cdk1 upon stable microtubule-kinetochore
216 attachments (*15, 28, 29*).
217
218 **References**

219 1. F. Verde, J. C. Labbé, M. Dorée, E. Karsenti, Regulation of microtubule dynamics by cdc2
220 protein kinase in cell-free extracts of Xenopus eggs. *Nature.* ***343,*** 233-238 (1990).
221 2. A. Lieuvin, J. C. Labbé, M. Dorée, D. Job, Intrinsic microtubule stability in interphase cells.
222 *J Cell Biol* **124**, 985-996 (1994).
223 3. N. Mchedlishvili, H. K. Matthews, A. Corrigan, B. Baum, Two-step interphase microtubule
224 disassembly aids spindle morphogenesis. *BMC Biol* ***16,*** 14 (2018).
225 4. Chang, W. et al. Phosphorylation of MAP4 affects microtubule properties and cell cycle
226 progression. J Cell Sci **114**, 2879-2887 (2001).
227 5. Vasquez ,R. J., Gard, D. L. & Cassimeris, L. Phosphorylation by CDK1 regulates XMAP215
228 function in vitro. *Cell Motil Cytoskeleton* **43**, 310-321 (1999).
229 6. Ookata, K. et al. Cyclin B interaction with microtubule-associated protein 4 (MAP4) targets
230 p34cdc2 kinase to microtubules and is a potential regulator of M-phase microtubule dynamics.
231 *J Cell Biol* **128**, 849-862 (1995).
232 7. Gergely, F., Draviam, V. M. & Raff, J. W. The ch-TOG/XMAP215 protein is essential for
233 spindle pole organization in human somatic cells. *Genes Dev* **17**, 336-341 (2003).
234 8. Hunt, T. On the regulation of protein phosphatase 2A and its role in controlling entry into and
235 exit from mitosis. *Adv Biol Regul* **53**, 173-178 (2013).

236 9. Krek, W. & Nigg, E. A. Mutations of p34cdc2 phosphorylation sites induce premature mitotic
237 events in HeLa cells: evidence for a double block to p34cdc2 kinase activation in vertebrates.
238 *EMBO J* **10**, 3331-3341 (1991).
239 10. D'Angiolella, V., Palazzo, L., Santarpia, C., Costanzo, V. & Grieco, D. Role for non-
240 proteolytic control of M-phase-promoting factor activity at M-phase exit. *PLoS One* **2**, e247
241 (2007).
242 11. Oh, J. S., Susor, A. & Conti, M. Protein tyrosine kinase Wee1B is essential for metaphase II
243 exit in mouse oocytes. *Science* **332**, 462-465 (2011).
244 12. Vassilev, L. T. et al. Selective small-molecule inhibitor reveals critical mitotic functions of
245 human CDK1. *Proc Natl Acad Sci U S A* **103** (2006).
246 13. Visconti, R. et al. The Fcp1-Wee1-Cdk1 axis affects spindle assembly checkpoint robustness
247 and sensitivity to antimicrotubule cancer drugs. *Cell Death Differ*. **22**, 1551-1560 (2015).
248 14. Serpico, A. F., D'Alterio, G., Vetrei, C., Della Monica, R., Nardella, L., Visconti, R. & Grieco,
249 D. Wee1 rather than Plk1 is inhibited by AZD1775 at therapeutically relevant concentrations.
250 *Cancers* **11**, 819 (2019).
251 15. Serpico, A. F. & Grieco, D. Recent advances in understanding the role of Cdk1 in the Spindle
252 Assembly Checkpoint. *F1000Res* **9**, F1000 Faculty Rev-57 (2020).
253 16. Silljé, H. H. W. & Nigg, E. A. Purification of mitotic spindles from cultured human cells.
254 *Methods* **38**, 25-28 (2006).
255 17. David, A. F. et al. Augmin accumulation on long-lived microtubules drives amplification and
256 kinetochore-directed growth. *J Cell Biol* **218**, 2150-2168 (2019).
257 18. Thawani, A. et al. The transition state and regulation of γ-TuRC-mediated microtubule
258 nucleation revealed by single molecule microscopy. *Elife* **9**, e54253. (2020).
259 19. Solomon, M. J., Lee, T. & Kirschner, M. W. Role of phosphorylation in p34cdc2 activation:
260 identification of an activating kinase. *Mol Biol Cell* **3**, 13-27 (1992).
261 20. Novák, B. & Tyson, J. J. Mechanisms of signalling-memory governing progression through
262 the eukaryotic cell cycle. *Curr Opin Cell Biol.* **69**, 7-16 (2021).
263 21. Pomerening, J. R., Sontag, E. D. & Ferrell, J. E. Jr. Building a cell cycle oscillator: hysteresis
264 and bistability in the activation of Cdc2. *Nat Cell Biol.* **5**, 346-351 (2003).
265 22. Ookata, K. et al. MAP4 is the in vivo substrate for CDC2 kinase in HeLa cells: identification
266 of an M-phase specific and a cell cycle-independent phosphorylation site in MAP4.
267 *Biochemistry* **36**, 15873-15883 (1997).

23. Charrasse, S., Lorca, T., Dorée, M. & Larroque, C. The Xenopus XMAP215 and its human homologue TOG proteins interact with cyclin B1 to target p34cdc2 to microtubules during mitosis. *Exp Cell Res* **254**, 249-256 (2000).
24. Kwon, Y. G., Lee, S. Y., Choi, Y., Greengard, P. & Nairn, A. C. Cell cycle-dependent phosphorylation of mammalian protein phosphatase 1 by cdc2 kinase. *Proc Natl Acad Sci U S A* **94**, 2168-2173 (1997).
25. Meadows, J. C. et al. Spindle checkpoint silencing requires association of PP1 to both Spc7 and kinesin-8 motors. *Dev Cell* **20**, 739-750 (2011).
26. Visconti, R., Palazzo, L., Della Monica, R. & Grieco, D. Fcp1-dependent dephosphorylation is required for M-phase-promoting factor inactivation at mitosis exit. *Nat Commun* **3**, 894 (2012).
27. Woodruff, J. B., et al. The centrosome is a selective condensate that nucleates microtubules by concentrating tubulin. *Cell* **169**, 1066-1077 (2017).
28. Yim, H. & Erikson R. L. Cell division cycle 6, a mitotic substrate of polo-like kinase 1, regulates chromosomal segregation mediated by cyclin-dependent kinase 1 and separase. *Proc Natl Acad Sci U S A* **107**,19742-19747 (2010).
29. Schmidt, A. K. et al. The p53/p73 - p21^{CIP1} tumor suppressor axis guards against chromosomal instability by restraining CDK1 in human cancer cells. *Oncogene* **40**, 436-451 (2021).

Acknowledgements

The authors acknowledge V. E. Avvedimento for suggestions, R. Visconti and A. Romano for technical advice. D.G. acknowledges AIRC, Associazione Italiana per la Ricerca sul Cancro, for support (IG grant 2017; Id. 19851 to D.G.).

Author contributions

A.F.S. and D.G. designed and performed experiments and analyzed data. C.P. and F.F. performed immunoblot and immunofluorescence experiments and analyzed data. D. G. wrote the manuscript. A.F.S. revised the manuscript. All authors read and approved the final manuscript.

Competing interests

The authors declare that they have no conflict of interest.

Figures

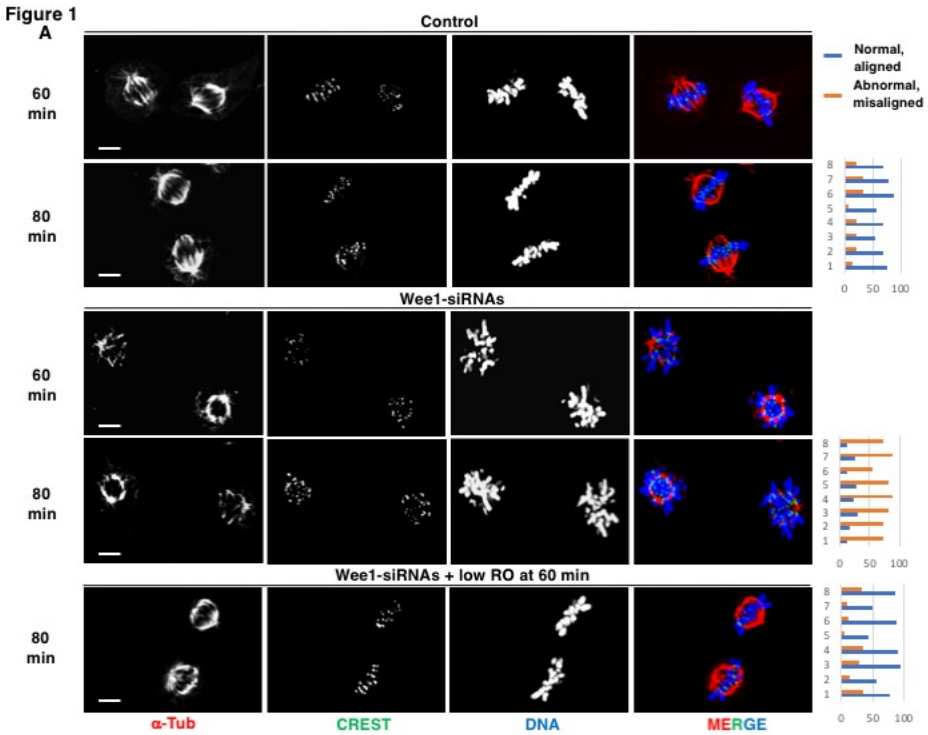

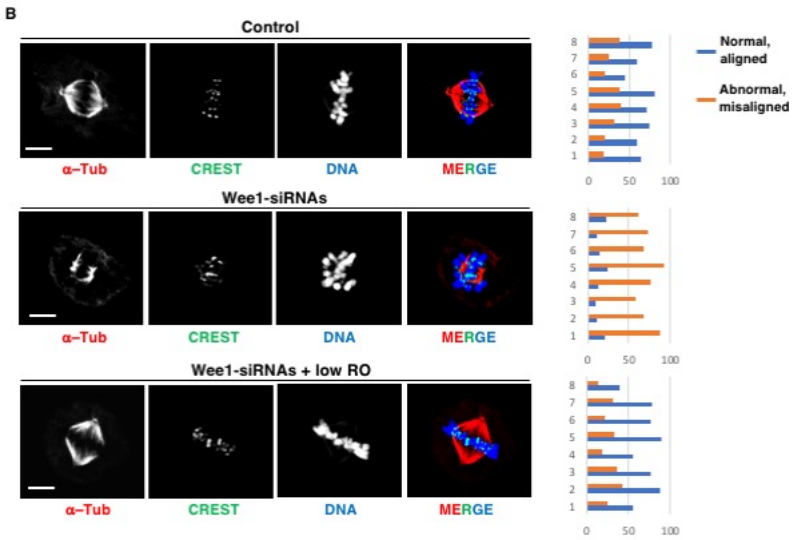

Fig. 1. Wee1 downregulation affects spindle assembly. (**A**) hTERT-RPE1 cells were arrested at G2 by high-RO treatment, released and fixed at 60 and 80 min of incubation in M/C medium (see Methods section). Control: Wee1-siRNA-treated cells previously transfected with siRNA-resistant Wee1 expression vector; Wee1-siRNAs: Wee1-siRNA-treated cells previously transfected with

empty vector; Wee1-siRNAs + low-RO: Wee1-siRNAs to which low-RO was added by 60 min from G2-arrest release. (**B**) hTERT-RPE1 cells were arrested at prometaphase with nocodazole, released and fixed after 80 min of incubation in M/C medium (see Materials and Methods). Control: cells treated with non-targeting siRNAs; Wee1-siRNAs: just Wee1-siRNA-treated cells; Wee1-siRNAs + low-RO: Wee1-siRNA-treated cells to which low-RO was added by 60 min from prometaphase-arrest release. Cells were fixed and stained for CREST (centromere marker, green), α-tubulin (α-Tub, red) and DNA (blue). Addition of vehicle (DMSO) had no effect on spindle assembly in Wee1-siRNA-treated cells. Graphs: quantitation of cells containing normal aligned (blue bar) or abnormal misaligned (orange bar) spindles at 80 min incubation; shown are data from two independent experiments (1-4, experiment 1; 5-8, experiment 2), around 100 cells were scored in 4 independent microscopy slide fields. Scale bar: 5 μm.

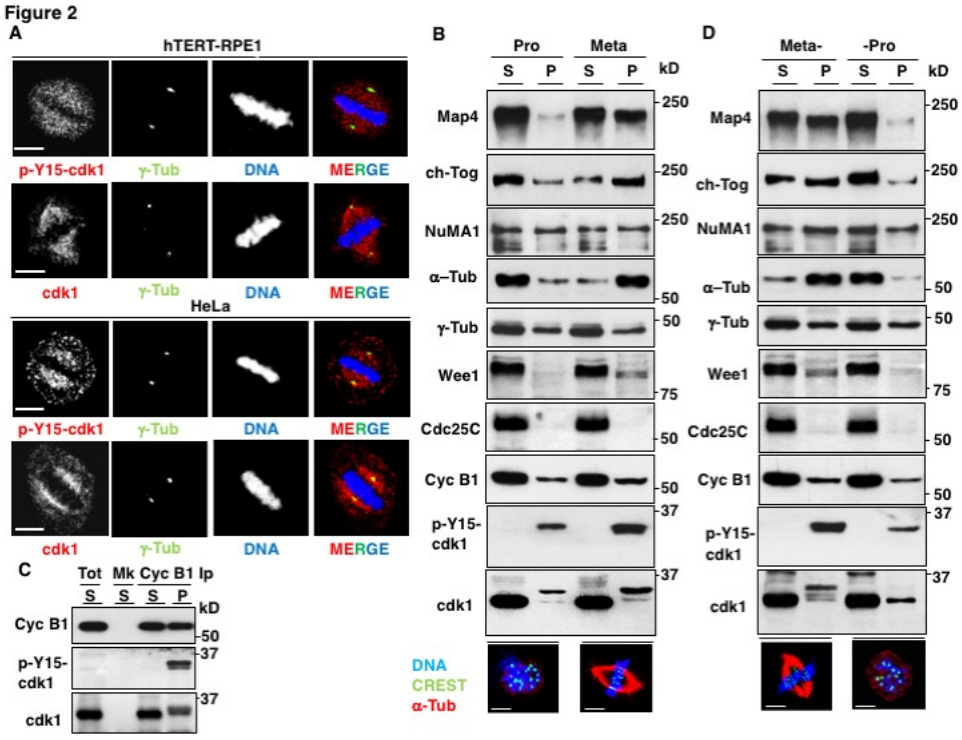

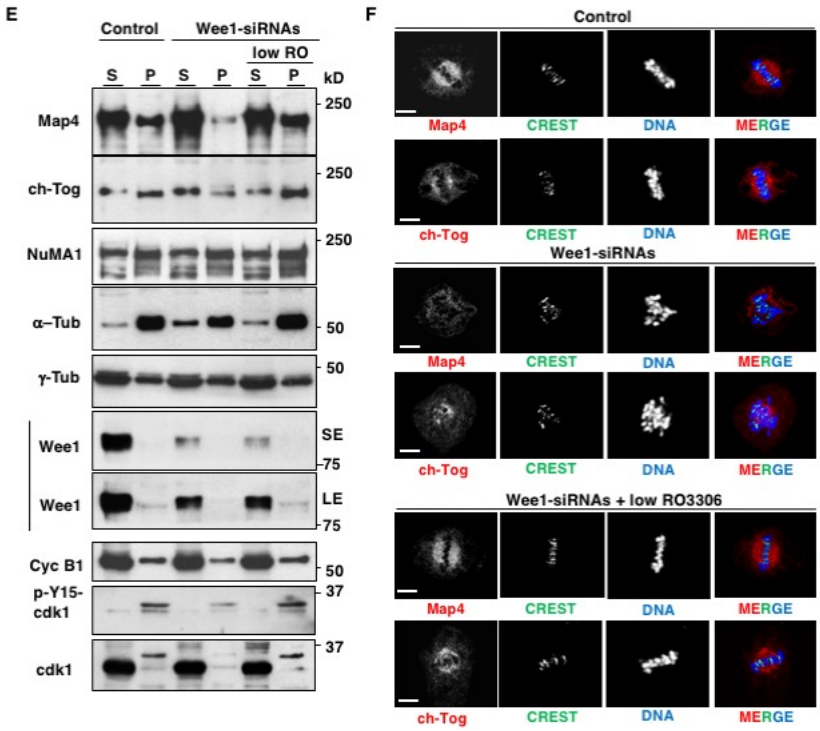

Fig. 2. i-Cdk1 localizes at spindle structures and is required for spindle assembly. (**A**) Growing hTERT-RPE1 and HeLa cells were treated for 20 min with MG-132, fixed and stained for indicated antigens (γ-Tub; γ-tubulin). (**B**) Prometaphase-arrested hTERT-RPE1 cells were released in M/C medium for 60 min and either nocodazole was added back at time 0 of incubation (Pro), or just vehicle (Meta). S and P fractions were probed for indicated antigens. Bottom: IFs of representative cells probed for indicated antigens. (**C**) Cyclin B1 Ips from Meta cell S and P fractions probed for indicated antigens. (**D**) Meta cells obtained as described in (B) were further treated with vehicle (Meta-) or nocodazole (-Pro) from 60 min to 80 min of incubation. S and P fractions were probed for indicated antigens. (**E**, **F**) hTERT-RPE1 cells were treated with non-targeting-siRNAs (Control) and Wee1-siRNAs, prometaphase-arrested and released in M/C medium for 80 min incubation as described in Fig. 1b and a portion of Wee1-siRNA-treated cells received low-RO at 60 min post release. (**E**) S and P fractions probed for indicated antigens; (**F**) Cells were fixed and stained for indicated antigens. Scale bar: 5 μm.

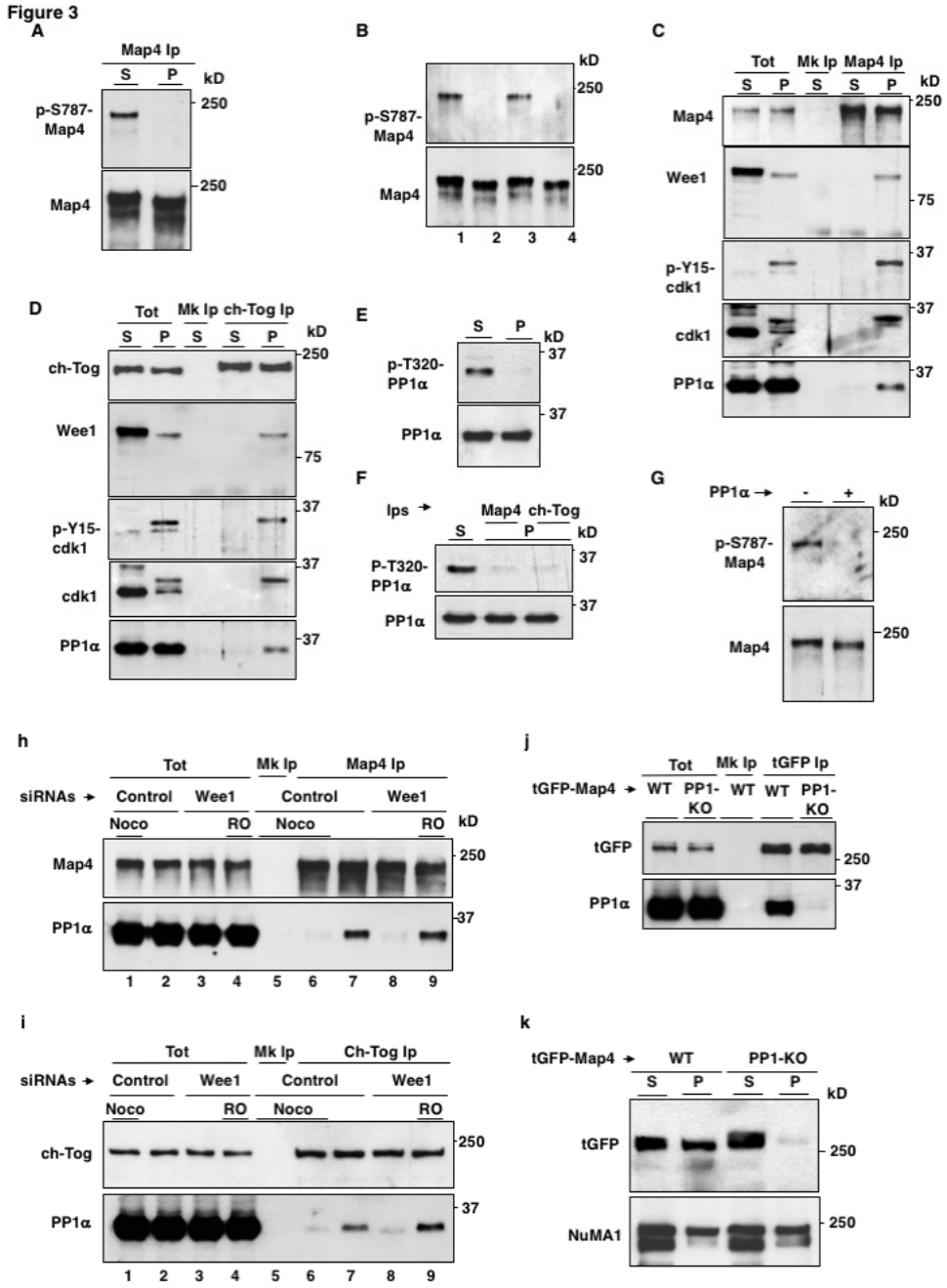

Fig. 3. i-Cdk1 assists spindle-localized MAP interaction with PP1 and dephosphorylation. From Meta hTERT-RPE1 cells: (**A**) Map4 Ips from S and P fractions were probed for indicated antigens. (**B**) Map4 Ips were incubated in kinase reaction buffer at 37° C for 15 min: lane 1, from S fraction; lanes 2, 3 and 4, from P fraction – or + active Cdk1 or + active Cdk1 + RO-3306, respectively. After incubation, Ips were probed for indicated antigens. (**C**) Map4 Ips and (**D**) ch-Tog Ips from S and P fractions were probed for indicated antigens. **e**, S and P fractions were probed for indicated antigens. (**F**) total S fraction and Map4 and ch-Tog Ips from P fraction were probed for indicated antigens. (**G**) Map4 Ips from S fraction were incubated in phosphatase reaction buffer at 37° C for 15 min in - or + active PP1α, then probed for indicated antigens. (**H**) and (**I**) Non-targeting-siRNA- (Control) and

350 Wee1-siRNA-treated (Wee1) hTERT-RPE1 cells released from prometaphase-arrest into M/C
351 medium for 80 min incubation. A sample of control cells received nocodazole at time 0 (Noco) and
352 a sample of Wee1-siRNAs cells received low-RO at 60 min of incubation (RO). Cells were lysed in
353 high salt buffer and (**H**) Map4 or (**I**) ch-Tog Ips were probed for indicated antigens (lanes 1-4, total
354 lysate; Mk Ip, mock Ips from Noco cell lysates). (**J**, **K**) hTERT-RPE1 cells were transfected with
355 tGFP-Map4-wild type (WT) and tGFP-Map4-PP1-KO expression vectors, arrested at metaphase and
356 either (J) lysed in high salt buffer, tGFP Ips were probed for indicated antigens or (K) S and P fraction
357 isolated and probed for indicated antigens.
358

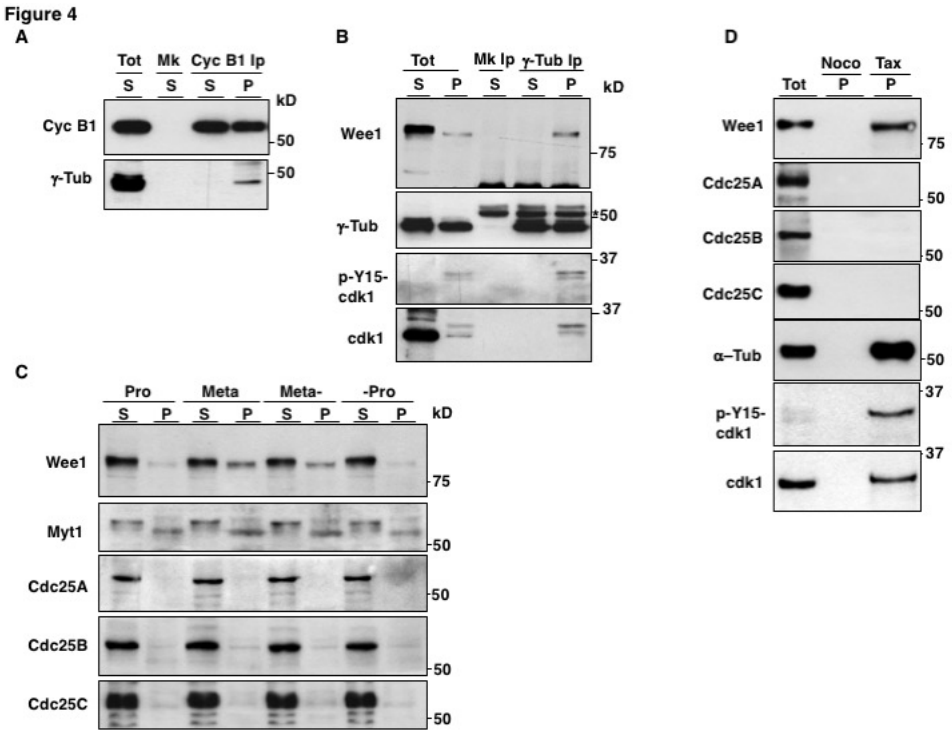

359

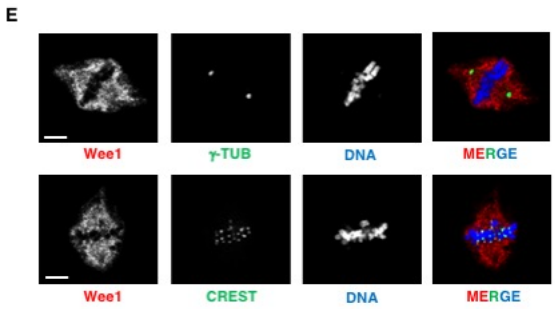

360
361
362
363
364
365

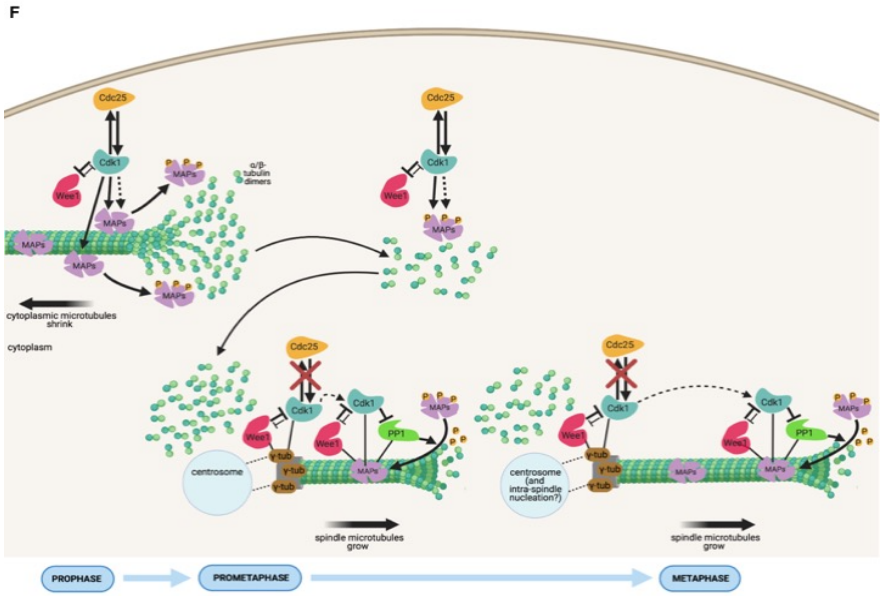

Fig. 4. Nucleating microtubules bind and foster i-Cdk1. (**A**) Cyclin B1 Ips described in fig. 2C were probed for γ-tubulin. (**B**) γ-tubulin Ips from S and P fraction of Pro hTERT-RPE1 cells were probed for indicated antigens (P fraction enriched 10 folds over S fraction). (**C**) S and P fraction from Pro, Meta, Meta- and -Pro, as described in Fig. 2b, d, were probed for indicated antigens on blots in which the P fraction was enriched 10 folds over S fraction. (**D**) Eluates from pellets of mitotic HeLa cell extracts (P) incubated with nocodazole (Noco) or taxol (Tax) were probed for indicated antigens; Tot: 1/20 of total extract. **E**, growing hTERT-RPE1 cells were treated for 20 min with MG-132, fixed and stained for indicated antigens. Scale bar: 5 μm. **(F**) a synoptic scheme depicting Cdk1 activity control in mitosis. At prophase, Cdk1 activity, sustained by positive feedback loops in the cytoplasm, destabilizes cytoplasmic microtubules by directly (continuous arrow) or indirectly (dotted arrow) phosphorylating MAPs. Centrosomes, however, maintain/promote inhibitory phosphorylation of a small Cdk1 fraction by selectively interacting with Wee1 and excluding Cdc25. From prometaphase to metaphase, further interaction of Wee1, inhibited Cdk1 and active PP-1 with microtubule-stabilizing MAPs expands from centrosomes, and possibly from intra-spindle γ-tubulin-dependent nucleating centers, to promote reversal of inhibitory MAP phosphorylation and spindle microtubule growth.

Supplementary Materials

Materials and Methods

389 **Cell lines and cell culture**

390 HeLa cells were grown in Roswell Park Memorial Institute Medium (RPMI-1640; Sigma-Aldrich),
391 hTERT-RPE1 cells were grown in Dulbecco's Modified Eagle Medium: Nutrient Mixture F-12
392 (DMEM/F12; Gibco, Thermo Fisher Scientific), both supplemented with 10% fetal bovine serum
393 (FBS; Gibco), 1% GlutaMAX-supplement (Gibco), 1% penicillin/streptomycin (Euroclone), at 37°
394 C with 5% CO_2.

395

396 **Cell treatments**

397 Transfections were performed using linear polyethylenimine (PEI; Polysciences, Inc) or MegaTran
398 2.0 Transfection Reagent (OriGene Technologies, Inc.). The expression plasmids for turbo-GFP-
399 Map4-wild type (tGFP-Map4-WT), turbo-GFP-Map4 rendered non-phosphorylatable at serine 787
400 (tGFP-Map4-S787A) and turbo-GFP-Map4 defective in PP1 binding Map4 (tGFP-Map4-PP1-KO),
401 in which the Map4 peptide KDVRW (from aa 318 to 32; human Map4 isoform 1) was mutated into
402 KDARA, were generated and purchased from OriGene Technologies Inc. Cdk1WT and cdk1AF
403 expression plasmids were purchased from Addgene. 3XFlag-Wee1 expression construct was obtained
404 as described[13]. SiRNAs targeting the 3′-UTR of human WEE1 (5′-GGGCUUU
405 AUUACAGACAUAUU-3′, 5′-GUACAUAGCUGUUUGAAAUUU-3′ and 5′-
406 UGUAAACUUGUAGCAUUAUU-3′) were purchased from Dharmacon Inc. For efficient
407 knockdown cells were transfected with 25 nM of siRNAs duplex using DharmaFECT 1 siRNA
408 Transfection Reagent (Dharmacon Inc.). For siRNA treatment and complementation experiments in
409 synchronized cells, cells were mock- or 3XFlag-Wee1 expression construct-transfected 24 hours prior
410 to treatment with non-targeting or specific siRNAs. For synchronization of siRNA-treated cells, 6
411 hours after siRNA-treatment, cells were incubated with RO-3306 at 9 μM (high-RO; Calbiochem)
412 for further 16 hours of incubation, to have G2-arrsted cells, or with nocodazole (Abcam) at 1 μg/ml
413 and 100 ng/ml for further 16 or 14 hours of incubation for hTERT-RPE1 and HeLa cells, respectively,
414 to have prometaphase-arrested cells (Pro cells). To obtain metaphase-arrested cells (Meta cells), Pro
415 cells were collected and washed twice with fresh medium and twice with phosphate buffer saline
416 (PBS; Euroclone) solution before plating into fresh medium containing MG-132 (20 μM;
417 Calbiochem) and cycloheximide (CHX; 60 μg/ml; Santa Cruz Biotechnology, Inc) for further 60 min
418 incubation. Meta- and -Pro cells were obtained by adding either DMSO or nocodazole (1 μg/ml) to
419 Meta cells at 60 min and prolonging incubation for further 20 min. Where indicated AZD1775
420 (Selleckchem) was added at 1 μM. Where indicated, partial reversal of Cdk1 activity was obtained
421 by adding RO-3306 at 0.5 μM (low-RO).

422

423 **Cell fractionation and extracts**

424 To isolate spindle-bound protein we adapted a previously described method[15]. All the steps, except
425 the final elution, were performed at room temperature (rt) to preserve microtubules. Cells were
426 harvested by centrifugation and washed once with PBS containing taxol (1 μM; Sigma-Aldrich). 5 x
427 10^6 cells were resuspended in 800 μl of fractionation lysis buffer (FLB; 40 mM β-glycerophosphate,
428 15 mM $MgCl_2$, 20 mM EGTA, 0,25% Igepal, 20 mM Hepes, 5 μM taxol, 6 μg/ml latrunculin B;
429 Sigma-Aldrich) supplemented with 300 μg/ml RNase A and 120 U/ml DNase I (Roche). After careful
430 resuspension, samples were incubated in thermomixer (Eppendorf thermomixer comfort) at 34 °C for
431 20 min with constant shaking at 1,200 rpm. Lysates were spun at 6,800 rpm (Eppendorf centrifuge
432 5425) for 2 min: the supernatant fractions were collected and transferred into new tubes and
433 supplemented with 250 mM NaCl (S fraction), the pellet fractions were resuspended in FLB + 300
434 μg/ml RNase A and 120 U/ml DNase I and again incubated in thermomixer at 34 °C for 20 min with
435 constant shaking at 1,200 rpm. Lysates were collected again by centrifugation and the pellets were
436 washed twice with washing buffer (WB; 5 mM Hepes, 5 μM taxol). Finally, the pellet fractions were
437 resuspended in 200 μl of FLB minus taxol and supplemented with 250 mM NaCl (P fraction). Both
438 supernatant and pellet fractions were incubated on ice, to help destabilize microtubules, for 30 min
439 and then spun at 3,200 rpm at 4 °C for 10 min (Eppendorf centrifuge 5424 R) and the supernatants of
440 S and P fraction further analyzed by Ibs or Ips. To induce microtubule polymerization and analyze
441 microtubule-bound proteins in mitotic cell extracts, HeLa cell extracts were obtained as previously
442 described[24]. Cell extracts were supplemented with 1 mM GTP (Sigma-Aldrich), 50 μl aliquots were
443 treated with nocodazole (1μg/ml; Abcam), as control, or taxol (5 μM; Sigma-Aldrich) for 20 min at
444 rt, diluted 10 times with FLB and spun at 6,800 rpm (Eppendorf centrifuge 5425) for 2 min. The
445 pellets were washed once more in FLB and finally resuspended in 30 μl FLB supplemented with 250
446 mM NaCl, incubated on ice for 30 min and then spun 13,200 rpm at 4 °C for 10 min (Eppendorf
447 centrifuge 5424 R). Supernatants were analyzed by Ibs; total samples = 5 μl of total mitotic extract.
448

449 **Antibodies**

450 Antibodies used for immunoblotting according to standard protocols: mouse anti-cdc2 (1:500; BD
451 Biosciences), rabbit anti-phospho-tyrosine-15-cdc2 (P-Y15-cdc2; 1:1000; Boster Bio), rabbit anti-
452 phospho-threonine-14-cdc2 (P-T14-cdc2; 1:1000; Cell Signaling Technology Inc.; CST), rabbit anti-
453 Wee1 (1:1000; CST), rabbit anti-Myt1 (1:1000; CST), rabbit anti-Cdc25C (1:1000; CST), rabbit anti-
454 phospho-threonine-320-PP1α (P-T320-PP1; 1:1000; CST), rabbit anti-cyclin B1 (1:2000; Bethyl
455 Laboratories, Inc.), mouse anti-γ-tubulin (1:2000; Sigma-Aldrich), mouse anti- α-tubulin (1:2000;

456 Sigma-Aldrich), mouse anti-PP1γ (1:500; Santa Cruz Biotechnology, Inc.), rabbit anti-Map4 (1:2000;
457 Bethyl Laboratories Inc.), rabbit anti-NuMA (1:1000; Novus Biologicals), rabbit anti-ch-Tog
458 (1:1000; Abcam), mouse anti-turboGFP (1:2000; OriGene Technologies). Rabbit polyclonal antibody
459 against phosphorylate serine 787 of human Map4 (P-S787-Map4) was raised using C-
460 DAKAPEKRA[Sp]PSKPA-coNH2 peptide as immunogen; peptide synthesis, rabbit inoculation,
461 serum production and cross-affinity antibody purification were carried out by CovalAb S.A.S. Sheep
462 anti-mouse IgG peroxidase-(HRP) linked and donkey anti-rabbit IgG HRP-linked whole antibodies
463 (1:2000; GE Healthcare). Antibodies used for IF: rabbit anti-phospho-tyrosine-15-cdc2 (P-Y15-cdc2;
464 1:50; CST), anti-cdc2 (1:100; BD Biosciences), mouse anti-γ-tubulin (1:1000; Sigma-Aldrich),
465 mouse anti-α-tubulin (1:1000; Sigma-Aldrich), rabbit anti-γ-tubulin (1:1000; Sigma-Aldrich), human
466 anti-centromere (CREST; 1:50; Antibodies Incorporated), rabbit anti-Map4 (1:1000; Abcam), rabbit
467 anti-ch-Tog (1:400; Proteintech Group, Inc.), rabbit anti-Wee1 (1:100; CST), goat anti-human IgG
468 rhodamine conjugated (4 µg/ml; Santa Cruz Biotechnology, Inc.), rabbit anti-human IgG FITC
469 conjugated (4 µg/mL; Dako Agilent), Alexa Fluor 594 donkey anti-rabbit IgG (2 µg/mL; Invitrogen),
470 Alexa Fluor 594 donkey anti-mouse IgG (4 µg/ml; Invitrogen), Alexa Fluor 488 donkey anti-rabbit
471 IgG (2 µg/ml; Invitrogen), Alexa Fluor 488 goat anti-mouse IgG (4 µg/ml; Invitrogen). Antibodies
472 used for Ips: rabbit anti-Map4 (2µg/mL; Bethyl Laboratories Inc.), rabbit anti-chTOG (2µg/mL;
473 Abcam), mouse anti-γ-tubulin (2µg/mL; Sigma-Aldrich). Antibody-conjugated beads used for Ips:
474 mouse anti-cyclin B1 agarose (Santa Cruz Biotechnology), mouse anti-turboGFP agarose (OriGene),
475 protein A/G PLUS-agarose (Santa Cruz Biotechnology), mouse anti-γ-tubulin agarose conjugate
476 (Santa Cruz Biotechnology).
477
478 **Immunoblotting and immunoprecipitation**
479 Immunoblots (Ib) were performed as described[26]. For immunoprecipitations (Ips) from S fraction and
480 and P fraction eluates, samples were diluted 6 folds in lysis buffer (LB; 80 mM β-glycerophosphate,
481 15 mM $MgCl_2$, 20 mM EGTA, 20 mM Hepes pH 7.4, 100 mM NaCl, 0,1 % Igepal; Sigma-Aldrich)
482 supplemented with 1 tablet of phosphatase inhibitor cocktail (PhosSTOP; Roche) and incubated with
483 antibody and protein A/G PLUS-agarose beads or with agarose bead-conjugated antibody overnight
484 at 4 °C in constant rotation. Beads were washed twice in LB and beads-bound proteins were eluted
485 by boiling in SDS loading buffer. For total cell lysates, 5 x 10^6 cells were lysed in 180 µl high salt
486 lysis buffer (HSB; 16 mM β-glycerophosphate, 3 mM $MgCl_2$, 4 mM EGTA, 0,5 mM DTT, 20 mM
487 Hepes, 0,2 % Igepal, 250 mM NaCl; Sigma-Aldrich) supplemented with 1 tablet of phosphatase
488 inhibitor cocktail (PhosSTOP; Roche) to preserve phosphorylation. After 30 min incubation on ice,
489 lysates were spun at 13,200 rpm for 10 min at 4° C (Eppendorf centrifuge 5424 R). Cleared lysates

490 were incubated with antibody and protein A/G PLUS-agarose beads or with agarose bead-conjugated
491 antibody overnight at 4 °C in constant rotation. Beads were washed twice in LB and beads-bound
492 proteins were eluted by boiling in SDS loading buffer. For kinase reactions, after the two LB washes,
493 Ips were washed once in kinase reaction buffer (KRB; 80 mM β-glycerophosphate, 15 mM $MgCl_2$,
494 20 mM EGTA, 20 mM Hepes pH 7.4, 100 μM ATP; Sigma-Aldrich) and incubated for 20 min at 37°
495 C in KRB -/+ recombinant active Cdk1 (0.05 mg/ml; Sigma-Aldrich) and + active Cdk1 + RO-3306
496 (10 μM). For phosphatase reactions, after the two LB washes, Ips were washed once in phosphatase
497 reaction buffer (PRB; 20 mM Hepes pH 7.4, 150 mM NaCl, 1 mM DTT, 1 mM $MnCl_2$; Sigma-
498 Aldrich) and incubated in PRB -/+ 0.01 mg/ml recombinant human PP1α (Novus Biologicals) for 20
499 min at 30° C.
500
501 **Immunofluorescence staining and microscopy**
502 Cells were grown onto poly-D-lysine (0,1 mg/ml; Sigma-Aldrich) coated glass coverslips and treated
503 as described in the text. Before immunofluorescence (IF) procedure initiation, coverslips were
504 washed twice with PBS, then cells were fixed with 4 % paraformaldehyde (Sigma-Aldrich) in PBS
505 (Euroclone) for 10 min at rt and with a methanol (99,9 %; Exacta + Optech) additional step at -20° C
506 for 10 min, the latter except for α-tubulin staining. Cells were permeabilized with 0,25-0,5 % Triton
507 X-100 (Sigma-Aldrich) in PBS for 15-30 min, washed once with PBS and incubated with 3% bovine
508 serum albumin (BSA; Sigma-Aldrich) in PBS for 1 hour at rt. Coverslips were transferred into a
509 humidity chamber and incubated with primary antibodies in 1,5 % (w/v) BSA-PBS solution for 2-12
510 hour at 4° C. Samples were washed three times and incubated with fluorescently labelled secondary
511 antibodies, dissolved in 1,5 % BSA-PBS solution, for 1 hour at rt. DNA was stained with Hoechst
512 33258 (1 μg/ml; Invitrogen) by incubation for 10 min. Finally, samples were washed four times and
513 mounted with Mowiol 40-88 (Sigma-Aldrich) on a glass side. Fixed cells were observed using LSM
514 980 inverted confocal microscope (Zeiss) with a 63X/1,4 oil objective. Representative images were
515 obtained collecting 3 Z-stack series over 42 μm. The acquisitions were deconvoluted and projected
516 into one plane using the LAS-AF software.
517
518 **Statistics and reproducibility**
519 For quantitative analyses of immunofluorescence experiments investigators were blinded to sample
520 allocation. Metaphases were visually scored and those with more than three chromosomes falling
521 outside the two internal quarters of the interpolar distance were considered misaligned; around 100
522 cells were scored in 4 fields of each slide for each experimental condition; each experiment was

523 repeated 3-5 times with similar results. Experiments analyzed by immunoblotting were repeated 2-8
524 times with similar results.
525
526 **Supplementary Figures**
527

Figure S1

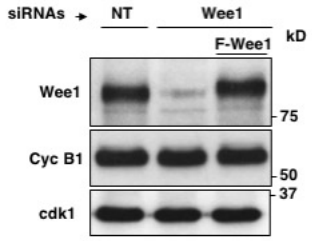

528
529 **Fig. S1. siRNAs treatment of hTERT-RPE1 cells.** Lysates of hTERT-RPE1 cells treated with non-
530 targeting siRNAs (NT) and with Wee1-siRNAs (Wee1) as described in fig.1 were probed for
531 indicated antigens. A portion of Wee1-siRNAs was previously transfected with a siRNAs-resistant,
532 Flag-tagged Wee1 expression vector (F-Wee1).
533

Figure S2

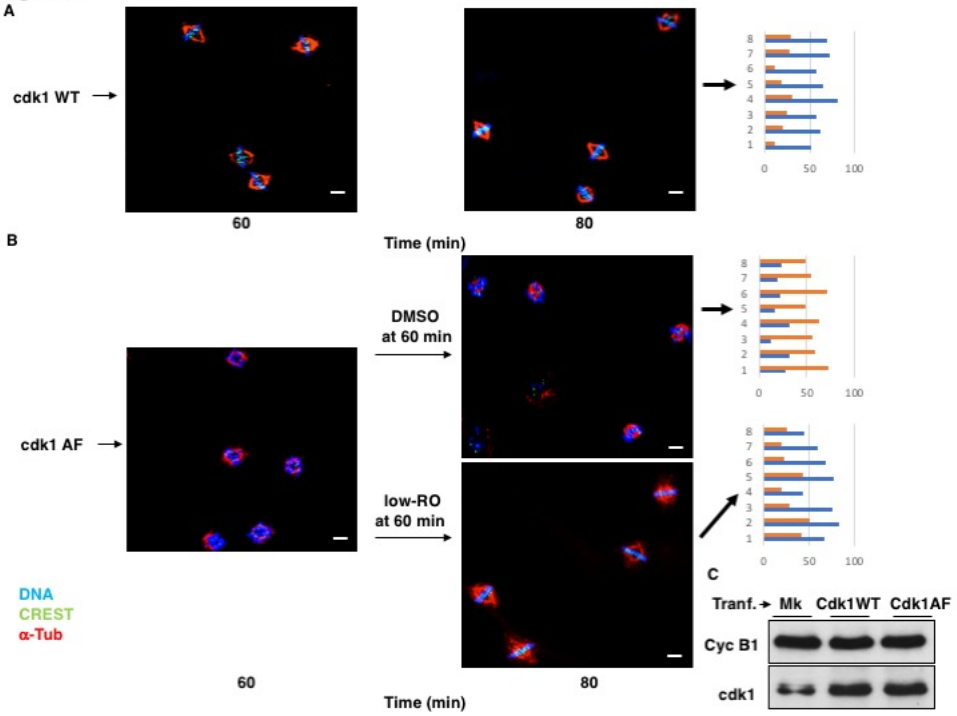

534
535 **Fig. S2. Expression of an inhibitory-phosphorylation-resistant version of Cdk1 impairs spindle**
536 **assembly.** hTERT-RPE1 cells were transfected with (**A**) wild type cdk1 (cdk1WT) expression vector

537 or (**B**) a mutant cdk1 expression vector in which cdk1-threonine 14 and tyrosine 15 are mutated into
538 non-phosphorylatable alanine and phenylalanine, respectively (cdk1AF). 6 hours post transfection,
539 cells were arrested at G2 by addition high-RO and for further 16 hours incubation. Cells were fixed
540 and stained for DNA (blue), α-tubulin (red) and CREST (green) at 60 and 80 min upon release from
541 G2 arrest. A portion of cdk1AF-transfected cells received low-RO at 60 min; as control vehicle was
542 added (DMSO). Graphs: quantitation of cells containing normal aligned (blue bar) or abnormal
543 misaligned (orange bar) spindles at 80 min incubation; shown are data from two independent
544 experiments, in which around 100 cells were scored in 4 independent microscopy slide fields (1-4,
545 experiment 1; 5-8, experiments 2). Scale bar: 5 µm. (**C**) samples of cells treated as in (A) and (B)
546 were lysed prior to release and probed for indicated antigens.
547

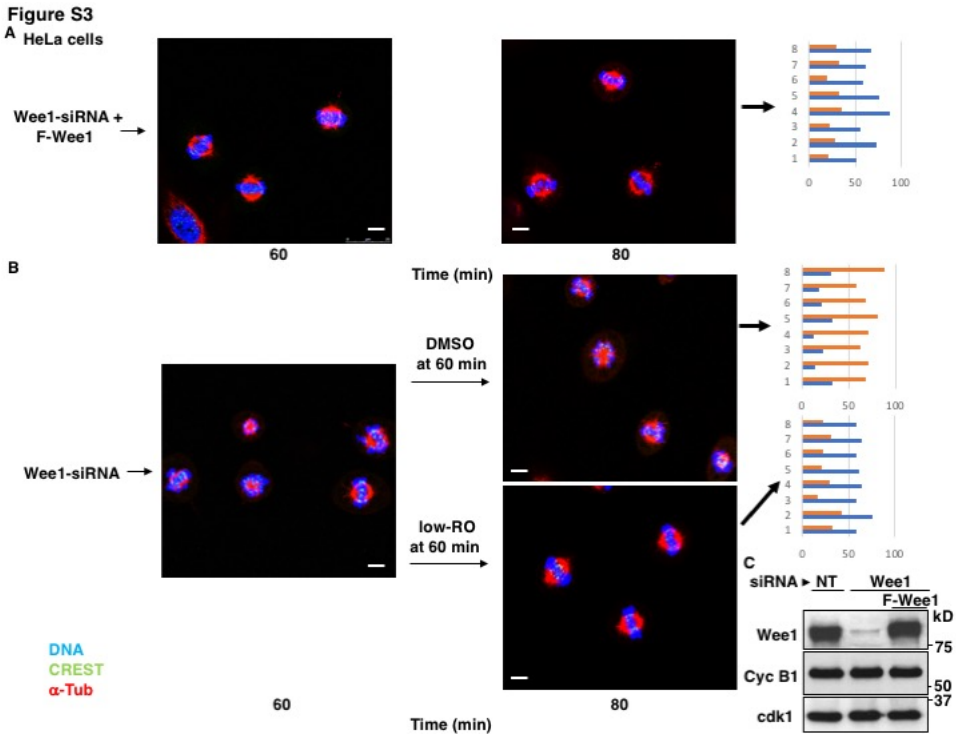

548
549

550 **Fig. S3. Downregulation of Wee1 impairs spindle assembly in HeLa cells.** HeLa cells were treated
551 and arrested at G2 as described for hTERT-RPE1 cells in Fig 1a. Cells were fixed and stained for
552 DNA (blue), α-tubulin (red) and CREST (green) at 60 and 80 min upon release from G2 arrest. (**A**)
553 Wee1-siRNA-treated cells complemented with siRNA-resistant expression vector (Wee1-siRNAs +
554 F-Wee1). (**B**) Wee1-siRNA-treated cells (Wee1-siRNAs). A portion of Wee1-siRNAs cells received
555 low-RO at 60 min; as control vehicle was added (DMSO). Graphs: quantitation of cells containing
556 normal aligned (blue bar) or abnormal misaligned (orange bar) spindles at 80 min incubation; shown
557 are data from two independent experiments, in which around 100 cells were scored in 4 independent

558 microscopy slide fields (1-4, experiment 1; 5-8, experiments 2). Scale bar: 5 µm. **c**, samples of cells
559 treated as in (A) and (B) were lysed prior to release and probed for indicated antigens.

Figure S4

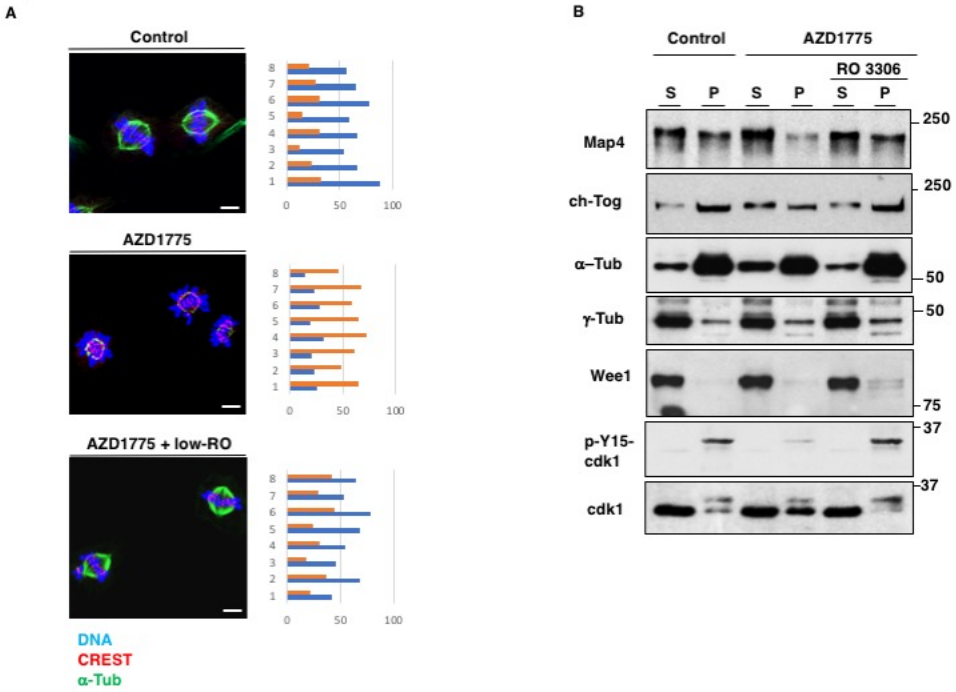

560

561 **Fig. S4. Chemical inhibition of Wee1 impairs spindle assembly.** (**A**) hTERT-RPE1 cells were
562 released from a G2 arrest by high-RO treatment into M/C medium and either vehicle (Control) or
563 AZD1775 was added. Cells were fixed after further 80 min of incubation and stained for α-tubulin
564 (green), centromeres (red) and DNA (blue). A sample of the AZD1775-treated cells also received
565 low-RO 60 min post release. Scale bar: 5 µm. (**B**) prometaphase-arrested hTERT-RPE1 were released
566 into M/C medium and either vehicle (Control) or AZD1775 was added. S and P fraction were
567 prepared after further 80 min of incubation and probed for indicated antigens. A sample of the
568 AZD1775-treated cells also received low-RO 60 min post release.

569

Figure S5

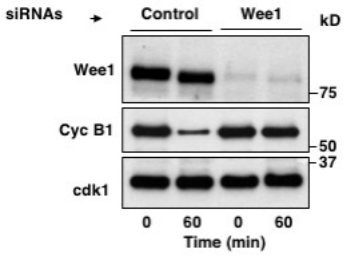

570

571 **Fig. S5. Downregulation of Wee1 delays mitosis exit.** Non-targeting-siRNA- (Control) or Wee1-
572 siRNA-treated (Wee1) hTERT-RPE1 cells were arrested at prometaphase and released into fresh
573 medium for 60 min of incubation. Cells were lysed and probed for indicated antigens.

574

Figure S6

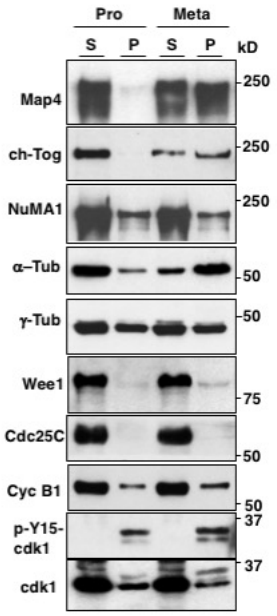

575

576 **Fig. S6. Mitotic HeLa cell fractionation.** Prometaphase-arrested HeLa cells were collected and
577 taken immediately (Pro) or released in M/C medium for 60 min (Meta). Fractionated S and P fractions
578 were probed for indicated antigens (P fraction enriched 4 folds over S fraction).

579

Figure S7

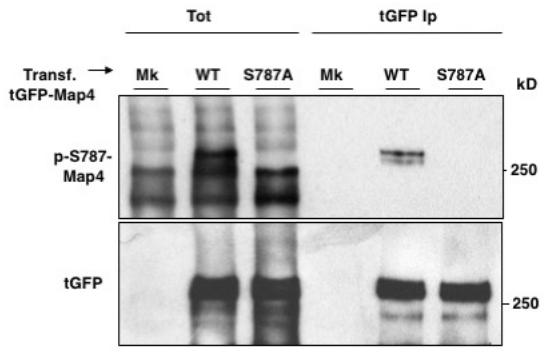

580

581 **Fig. S7. Detection of S787-Map4 phosphorylation.** hTERT-RPE1 cells were transfected with
582 expression vectors of tGFP-Map4 wild type (WT) or tGFP-Map4 mutant version in which serine 787
583 of Map4 was mutated into alanine (S787A) and arrested at prometaphase. Total cell lysates (Tot) and
584 relative anti-tGFP Ips were probed for indicated antigens (Mk: mock-transfected cells).

585

586